The spectroscopic characterization, photochromism of cadmium(II)–iodo complexes of 1-alkyl-2-(arylazo)imidazoles and DFT computation of representative complexes

ARTICLE *in* SPECTROCHIMICA ACTA PART A MOLECULAR AND BIOMOLECULAR SPECTROSCOPY · SEPTEMBER 2014

Impact Factor: 2.35 · DOI: 10.1016/j.saa.2014.08.094 · Source: PubMed

6 AUTHORS, INCLUDING:

Debashis Mallick
Mrinalini Datta Mahavidyapith
12 PUBLICATIONS **35** CITATIONS

SEE PROFILE

Spectrochimica Acta Part A: Molecular and Biomolecular Spectroscopy 137 (2015) 935–944

Contents lists available at ScienceDirect

Spectrochimica Acta Part A: Molecular and Biomolecular Spectroscopy

journal homepage: www.elsevier.com/locate/saa

The spectroscopic characterization, photochromism of cadmium(II)-iodo complexes of 1-alkyl-2-(arylazo)imidazoles and DFT computation of representative complexes

Chandana Sen, Avijit Nandi, Debashis Mallick [1], Sudipa Mondal, Kamal Krishna Sarker [2], Chittaranjan Sinha *

Department of Chemistry, Inorganic Chemistry Section, Jadavpur University, Kolkata 700 032, India

HIGHLIGHTS

- Two series of complexes $[Cd(RaaiC_nH_{2n+1})(\mu\text{-}I)(I)]_2$ and $[Cd(Raai\text{-}C_nH_{2n+1})_2I_2]$ are characterized.
- Coordinated $RaaiC_nH_{2n+1}$ show E-to-Z photoisomerisation upon UV light irradiation.
- Z-to-E isomerisation is achieved by thermal route and activation energy is calculated.
- Quantum yields of photochromism of coordinated $Raai\text{-}C_nH_{2n+1}$ are lower than free ligand.
- DFT optimized structures and molecular functions are used to explain spectral data.

GRAPHICAL ABSTRACT

$[Cd(Raai\text{-}C_nH_{2n+1})(\mu\text{-}I)I]_2$ and $[Cd(Raai\text{-}C_nH_{2n+1})_2I_2]$ ($Raai\text{-}C_nH_{2n+1}$, 1-alkyl-2-(arylazo)imidazole, $n = 4, 6, 8$) are spectroscopically characterized. The coordinated $Raai\text{-}C_nH_{2n+1}$ shows photochromism, E(*trans*)-to-Z(*cis*) isomerisation, upon UV light irradiation. The reverse process, Z-to-E is very slow in visible light irradiation process while the reaction is sensitive to change of reaction temperature. The quantum yields ($\phi_{E\to Z}$) for E-to-Z and the activation energy (E_a) of Z-to-E isomerisation are calculated and found that the complexes show subordinate results compared to free ligand. DFT optimized structures of representative complexes have been generated and the molecular functions have been used to explain the spectral and photochromic phenomena.

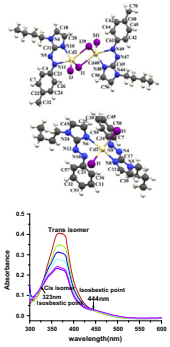

ARTICLE INFO

Article history:
Received 19 June 2014
Received in revised form 11 August 2014
Accepted 24 August 2014
Available online 4 September 2014

Keywords:
Cadmium(II)
Arylazoimidazoles

ABSTRACT

$[Cd(Raai\text{-}C_nH_{2n+1})(\mu\text{-}I)I]_2$ and $[Cd(Raai\text{-}C_nH_{2n+1})_2I_2]$ are synthesized by the reaction of CdI_2 with 1-alkyl-2-(arylazo)imidazole ($Raai\text{-}C_nH_{2n+1}$, $n = 4, 6, 8$) in MeOH in 1:1 and 1:2 M ratio of salt and ligands, respectively. The complexes have been characterized by spectral data (UV–Vis, IR, ^1H NMR, Mass). The coordinated $Raai\text{-}C_nH_{2n+1}$ shows photochromism, E(*trans*)-to-Z(*cis*) isomerisation, upon UV light irradiation. The reverse process, Z-to-E, is very slow in visible light irradiation process while the reaction is sensitive to change of reaction temperature. The quantum yields ($\phi_{E\to Z}$) for E-to-Z and the activation energy (E_a) of Z-to-E isomerisation are calculated and found that the complexes show subordinate results compared

* Corresponding author. Fax: +91 2414 6584.
E-mail address: c_r_sinha@yahoo.com (C. Sinha).
[1] Present address: Department of Chemistry, Mrinalini Datta Mahavidyapith, Kolkata 700 051, India.
[2] Present address: Department of Chemistry, Mahadevananda Mahavidyalaya, Monirampore, Barrackpore, Kolkata 700 120, India.

http://dx.doi.org/10.1016/j.saa.2014.08.094
1386-1425/

Photochromism
Quantum yield
Activation energy
DFT computation

to free ligand. DFT computations of two representative complexes were carried out to explain the spectral and photochromic phenomena.

Introduction

Photochromism is the reversible transformation of a chemical species between two forms by the absorption of electromagnetic radiation, where the two forms have different absorption spectra [1,2]. 1-Alkyl-2-(arylazo)imidazoles (Raai-C_nH_{2n+1}) are eligible photochrome (Scheme 1) and undergo E-to-Z (*trans*-to-*cis*) isomerisation about —N=N— bond upon irradiation with UV light whereas the reverse transformation, Z-to-E (*cis*-to-*trans*), is very slow with visible light irradiation and has been carried out under thermal treatment [3–12]. During the isomerization of photochrome significant changes of properties like the absorption, molecular dimensions and dipole moment take place [13,14]. The change of properties has been used, in general, in information storage, optical switching devices, surface relief gratings, nonlinear optics, etc. [15–17]. Fatigue and low durability are main problems of organic photochrome which could be minimized by coordination with metal ions. For the last few years we are working on the photochromism of Raai-C_nH_{2n+1} and their metal complexes [3–12] in different microenvironments [18–20]. Non transition metal complexes show better efficiency towards photoisomerisation than transition metal complexes. The d^{10} electronic configuration of non transition metal complexes may assist excited energy transfer to execute bond inversion or rotation so that isomerisation may take place. In this article, we report the photoisomerisation of hitherto unknown Cd(II)-coordination complexes of 1-alkyl-2-(arylazo)imidazoles, Raai-C_nH_{2n+1} (n = 4, 6, 8). Two groups of complexes have been synthesized using the molar ratio of Cd(II): Raai-C_nH_{2n+1}; 1:1 molar ratio has isolated [Cd(Raai-C_nH_{2n+1})(μ-I)I]$_2$ and 1:2 M ratio gives [Cd(Raai-C_nH_{2n+1})$_2$I$_2$]. The structural characterization has been carried out by spectroscopic data (IR, UV–Vis, ^{1}H NMR, Mass). DFT computation of optimized geometries has been used to explain the photochromism of the complexes.

Experimental

Materials

1-Alkyl-2-(arylazo)imidazoles were synthesized by reported procedure [10]. 1-Bromo-nalkanes, C_nH_{2n+1}-1-Br, where n = 4, 6, 8 were purchased from Sigma–Aldrich and were of analytical reagent grade and used as received. CdI_2 was purchased from Merck and all other chemicals and solvents were reagent grade and used as received and the solvents were purified before use by standard procedure [12].

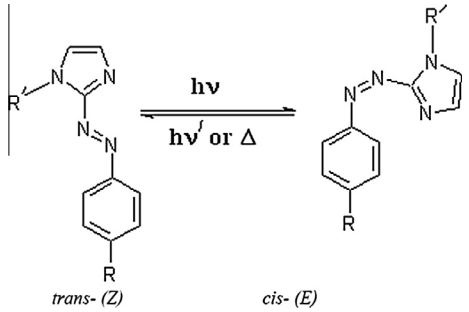

Scheme 1. Photoisomerisation of 1-alkyl-2-(arylazo)imidazole.

Physical measurements

Microanalytical data (C, H, N) were collected on Perkin–Elmer 2400 CHNS/O elemental analyzer. Spectroscopic data were obtained using the following instruments: UV–Vis spectra from a Perkin Elmer Lambda 25 spectrophotometer; IR spectra (KBr disk, 4000–400 cm^{-1}) from a Perkin Elmer RX-1 FTIR spectrophotometer; photo excitation has been carried out using a Perkin Elmer LS-55 spectrofluorimeter and ^{1}H NMR spectra were recorded from a Bruker (AC) 300 MHz FTNMR spectrometer. ESI mass spectra were recorded on a micro mass Q-TOF mass spectrometer (serial No. YA 263).

Synthesis of complexes

*[Cd(Meaai-C_6H_{13})(μ-I)I]$_2$ (**5b**)*

To methanol (10 ml) suspension of CdI_2 (0.30 g, 0.82 mmol) was added in drops of Meaai-C_6H_{13} (0.25 g, 0.93 mmol) in the same solvent and the mixture was stirred for 2 h. A dark orange precipitate appeared. It was filtered and washed with KI solution (2%). It was then washed with large volume of water and dried in desiccator ($CaCl_2$). Purification was carried out by recrystallization from 2-methoxyethanol–MeOH (1:3, v/v) mixture. It was dried in vacuum and preserved at dark. Yield 0.24 g (46%).

Following identical procedure, other complexes were prepared and yield varied 45–65%. Microanalytical and spectroscopic data are given below.

[Cd(Haai-C_4H_9)(μ-I)I]$_2$ (**4a**): Calculated for $C_{26}H_{32}N_8Cd_2I_4$: C, 26.28; H, 2.76; N, 9.42%; Found: C, 26.38; H, 2.91; N, 9.56%. m/z+, 593.85. ^{1}H NMR (300 MHz, $CDCl_3$) δ 7.35 (2H, bs, 4,4′H), 7.28 (2H, bs, 5,5′H), 7.82 (4H, d, 8.1 Hz, 7,7′,11,11′H), 7.52 (4H, t, 7.9 Hz, 8,8′,10,10′H), 7.54 (2H, t, 8.1 Hz, 9,9′H), 4.48 (4H, t,7.0 Hz, 12,12′CH_2), 0.93 (6H, t, 6.0 Hz, 15,15′CH_3), 1.89–1.34 (8H, m, 13–14,13′–14′CH_2). FT-IR (KBr, ν cm^{-1}) ν (N=N), 1412; ν (C=N), 1632; UV–Vis (λ_{max}, nm (ε, 10^3 M^{-1} cm^{-1}) in MeOH), 365 (26.28), 378 (20.45), 449 (2.8). [Cd(Meaai-C_4H_9)(μ-I)I]$_2$ (**4b**): Calculated for $C_{28}H_{36}N_8Cd_2I_4$: C, 27.63; H, 2.96; N, 9.26%; Found: C, 27.74; H, 2.82; N, 9.43%. m/z+, 607.90. ^{1}H NMR (300 MHz, $CDCl_3$) δ 7.42 (2H, bs, 4,4′H), 7.26 (2H,bs, 5,5′,H), 7.75 (4H, d, 8.1 Hz, 7,7′,11,11′H), 7.47 (4H, d, 7.6 Hz, 8,8′,10,10′H), 2.52 (6H, s,9,9′CH_3), 4.48 (4H, t,7.0 Hz, 12,12′CH_2), 0.93 (6H, t, 5.9 Hz, 15,15′CH_3), 1.87–1.34 (8H, m, 13–14,13′–14′CH_2). FT-IR (KBr, ν cm^{-1}) ν (N=N), 1414; ν (C=N), 1635; UV–Vis (λ_{max}, nm (ε, 10^3 M^{-1} cm^{-1}) in MeOH), 365 (27.22), 381 (21.78), 449 (3.2). [Cd(Haai-C_6H_{13})(μ-I)I]$_2$ (**5a**): Calculated for $C_{30}H_{40}N_8Cd_2I_4$: C, 28.87; H, 3.28; N, 9.04%; Found: C, 28.92; H, 3.46; N, 9.24%. m/z+, 621.92. ^{1}H NMR (300 MHz, $CDCl_3$) δ 7.45 (2H, bs, 4,4′H), 7.29 (2H, bs, 5,5′, H), 7.93 (4H, d,8.0 Hz, 7,7′,11,11′H), 7.49 (4H, t, 7.8 Hz, 8,8′,10,10′H), 7.45 (2H, t, 7.3 Hz, 9,9′H), 4.48 (4H, t,6.9 Hz, 12,12′CH_2), 0.93 (6H, t, 6.2 Hz, 15,15′CH_3), 1.89–1.34 (16H, m, 13–16,13′-16′CH_2). FTIR (KBr, ν cm^{-1}) ν (N=N), 1416; ν (C=N), 1632; UV–Vis (λ_{max}, nm (ε, 10^3 M^{-1} cm^{-1}) in MeOH),364 (26.39), 383 (20.93), 452 (3.3). [Cd(Meaai-C_6H_{13})(μ-I)I]$_2$ (**5b**): Calculated for $C_{32}H_{44}N_8Cd_2I_4$: C, 30.26; H, 3.54; N, 8.86%; Found: C, 30.42; H, 3.68; N, 8.98%. m/z+, 635.94. ^{1}H NMR (300 MHz, $CDCl_3$) δ 7.37 (2H, bs, 4,4′H),7.25 (2H, bs, 5,5′,H), 7.84 (4H, d, 9.2 Hz,7,7′,11,11′H), 7.36 (4H, d, 8.0 Hz, 8,8′,10,10′H), 2.48 (6H, s, 9,9′CH_3), 4.48 (4H, t, 7.1 Hz,12,12′CH_2), 0.92 (6H, t, 6.0 Hz, 17,17′CH_3), 1.90–1.35 (16H, m, 13–16,13′-16′CH_2). FT-IR(KBr, ν cm^{-1}) ν (N=N), 1409; ν

(C=N), 1633; UV–Vis (λ_{max}, nm (ε, $10^3\,M^{-1}\,cm^{-1}$) in MeOH), 366(27.38), 382 (21.37), 450 (3.0). [Cd(Haai-C_8H_{17})(μ-I)I]$_2$ (**6a**): Calculated for $C_{34}H_{48}N_8Cd_2I_4$: C,31.34; H, 3.74; N, 8.88%; Found: C, 31.46; H, 3.68; N, 8.98%. *m/z*+, 649.96. ^{1}H NMR (300 MHz, $CDCl_3$) δ 7.38 (2H, bs, 4,4′H), 7.24 (2H, bs, 5,5′,H), 7.94 (4H, d, 8.3 Hz, 7,7′,11,11′H),7.47 (4H, t, 8.0 Hz, 8,8′,10,10′H), 7.48 (2H, t, 6.9 Hz, 9,9′H), 4.52 (4H, t, 7.0 Hz,12,12′CH_2), 0.91 (6H, t, 6.7 Hz, 19,19′CH_3), 1.93–1.36 (24H, m, 13–18,13′-18′CH_2). FT-IR (KBr, ν cm^{-1}) ν (N=N), 1408; ν (C=N), 1632; UV–Vis λ_{max}, nm (ε, $10^3\,M^{-1}\,cm^{-1}$) in MeOH), 364 (27.66), 382 (22.04), 450 (3.2). [Cd(Meaai-C_8H_{17})(μ-I)I]$_2$ (**6b**): Calculated for $C_{36}H_{52}N_8Cd_2I_4$: C, 32.56; H, 3.90; N, 8.49% Found: C, 32.39; H, 3.77; N, 8.72%. *m/z*+, 664.04. ^{1}H NMR (300 MHz, $CDCl_3$) δ 7.35 (2H, bs, 4,4′H), 7.21 (2H, bs, 5,5′,H), 7.90 (4H, d, 7.6 Hz, 7,7′,11,11′H), 7.34 (4H, d, 7.9 Hz, 8,8′,10,10′H), 2.47 (6H, s, 9,9′CH_3), 4.48 (4H, t, 6.5 Hz,12,12′CH_2), 0.89 (6H, t, 6.0 Hz, 19,19′CH_3), 1.89–1.34 (24H, m, 13–18, 13′-18′CH_2). FT-IR (KBr, ν cm^{-1}) ν (N=N), 1415; ν (C=N), 1627; UV–Vis λ_{max}, nm (ε, $10^3\,M^{-1}\,cm^{-1}$) in MeOH), 367 (27.82), 383 (21.48), 445 (3.2).

*[Cd(Meaai-C_6H_{13})$_2$$I_2$] (**8b**)*

To methanol (10 ml) suspension of CdI_2 (0.30 g, 0.82 mmol) was added in drops of Meaai-C_6H_{13} (0.59 g, 2.20 mmol) in the same solvent and the mixture was stirred for 2 h. A dark orange precipitate appeared. It was filtered and washed with KI solution (2%). It was then washed with large volume of water and dried in desiccators ($CaCl_2$). Purification was carried out by recrystallization from 2-methoxyethanol–MeOH (1:3, v/v) mixture. It was dried in vacuum and preserved at dark. Yield 0.31 g (64%).

Following identical procedure, other complexes were prepared and yield varied 60–75%. Microanalytical and spectroscopic data are given below.

[Cd(Haai-C_4H_9)$_2$$I_2$] (**7a**): Calculated for $C_{26}H_{32}N_8CdI_2$: C, 37.89; H, 3.90; N, 13.60%; Found: C, 37.68; H, 3.98; N, 13.49%. *m/z*+, 695.13. ^{1}H NMR (300 MHz, $CDCl_3$) δ 7.34 (2H, bs, 4,4′H), 7.21 (2H, bs, 5,5′,H), 7.89 (4H, d, 7.6 Hz, 7,7′,11,11′H), 7.43 (4H, t, 7.4 Hz, 8,8′,10,10′H), 7.43 (2H, t, 7.2 Hz, 9,9′H), 4.51 (4H, t, 6.8 Hz, 12,12′CH_2), 0.88 (6H, t, 5.3 Hz, 15,15′CH_3), 1.90–1.35 (8H, m, 13–14,13′-14′CH_2). FT-IR (KBr, ν cm^{-1}) ν (N=N), 1412; ν (C=N), 1617; UV–Vis λ_{max}, nm (ε, $10^3\,M^{-1}\,cm^{-1}$) in MeOH), 367 (26.21), 381 (20.93), 449 (3.1). [Cd(Meaai-C_4H_9)$_2$$I_2$] (**7b**): Calculated for $C_{28}H_{36}N_8CdI_2$: C, 39.48; H, 4.18; N, 13.23%; Found: C, 39.57; H, 4.41; N, 13.45%. *m/z*+, 695.13. ^{1}H NMR (300 MHz, $CDCl_3$) δ 7.28 (2H, bs, 4,4′H), 7.16 (2H, bs, 5,5′,H),7.81 (4H, d, 7.9 Hz, 7,7′,11,11′H), 7.37 (4H, t, 7.4 Hz, 8,8′,10,10′H), 2.42 (6H, s, 9,9′CH_3), 4.42(4H, t, 6.9 Hz, 12,12′CH_2), 0.85 (6H, t, 5.8 Hz, 15,15′CH_3), 1.87–1.34 (8H, m, 13–14,13′-14′CH_2). FT-IR (KBr, ν cm^{-1}) ν (N=N), 1412; ν (C=N), 1609; UV–Vis λ_{max}, nm (ε, $10^3\,M^{-1}\,cm^{-1}$) in MeOH), 367 (25.57), 383 (22.68), 453 (2.7). [Cd(Haai-C_6H_{13})$_2$$I_2$] (**8a**): Calculated for$C_{30}H_{40}N_8CdI_2$: C, 41.26; H, 4.64; N, 12.79%; Found: C, 41.42; H, 4.79; N, 12.63%. *m/z*+, 751.62. ^{1}H NMR (300 MHz, $CDCl_3$) δ 7.64 (2H, bs, 4,4′H), 7.32 (2H, bs, 5,5′,H), 7.96 (4H, d,8.4 Hz, 7,7′,11,11′H), 7.48 (4H, t, 7.6 Hz, 8,8′,10,10′H), 7.42 (2H, t, 7.5 Hz, 9,9′H), 4.33 (4H, t,7.3 Hz, 12,12′CH_2), 0.89 (6H, t, 5.3 Hz, 17,17′CH_3), 1.80–1.67 (16H, m, 13–16,13′-16′CH_2). FTIR (KBr, ν cm^{-1}) ν (N=N), 1421; ν (C=N), 1615; UV–Vis λ_{max}, nm (ε, $10^3\,M^{-1}\,cm^{-1}$) in MeOH), 366 (27.23), 385 (23.03), 455(3.1). [Cd(Meaai-C_6H_{13})$_2$$I_2$] (**8b**): Calculated for $C_{32}H_{44}N_8CdI_2$: C, 42.41; H, 4.96; N, 12.39%; Found: C, 42.18; H, 4.73; N, 12.20%. *m/z*+, 779.15. ^{1}H NMR (300 MHz, $CDCl_3$) δ 7.33 (2H, bs, 4,4′H), 7.17 (2H, bs, 5,5′,H), 7.83 (4H, d, 8.3 Hz, 7,7′,11,11′H), 7.31 (4H, d, 7.4 Hz, 8,8′,10,10′H), 2.41 (6H, s, 9,9′CH_3), 4.45 (4H, t, 7.3 Hz, 12,12′CH_2), 0.85(6H, t, 6.1 Hz, 17,17′CH_3), 1.90–1.35 (16H, m, 13–16,13′-16′CH_2). FT-IR (KBr, ν cm^{-1}) ν (N=N), 1444; ν (C=N), 1590; UV–Vis λ_{max}, nm (ε, $10^3\,M^{-1}\,cm^{-1}$) in MeOH), 364 (26.38), 381 (25.38), 451 (2.9). [Cd(Haai-C_8H_{17})$_2$$I_2$] (**9a**): Calculated for $C_{34}H_{48}N_8CdI_2$: C, 43.71; H, 5.20; N, 11.93%; Found: C, 43.88; H, 5.36; N, 12.18%. *m/z*+, 807.96. ^{1}H NMR (300 MHz, $CDCl_3$) δ 7.37 (2H, bs, 4,4′H), 7.19 (2H, bs, 5,5′,H), 8.21 (4H, d, 8.0 Hz, 7,7′,11,11′H), 7.51 (4H, t, 7.4 Hz,8,8′,10,10′H), 7.49 (2H, t, 7.6 Hz, 9,9′H), 4.47 (4H, t, 7.3 Hz, 12,12′CH_2), 0.85 (6H, t, 6.2 Hz,19,19′CH_3), 1.92–1.36 (24H, m, 13–18,13′-18′CH_2). FT-IR (KBr, ν cm^{-1}) ν (N=N), 1400;

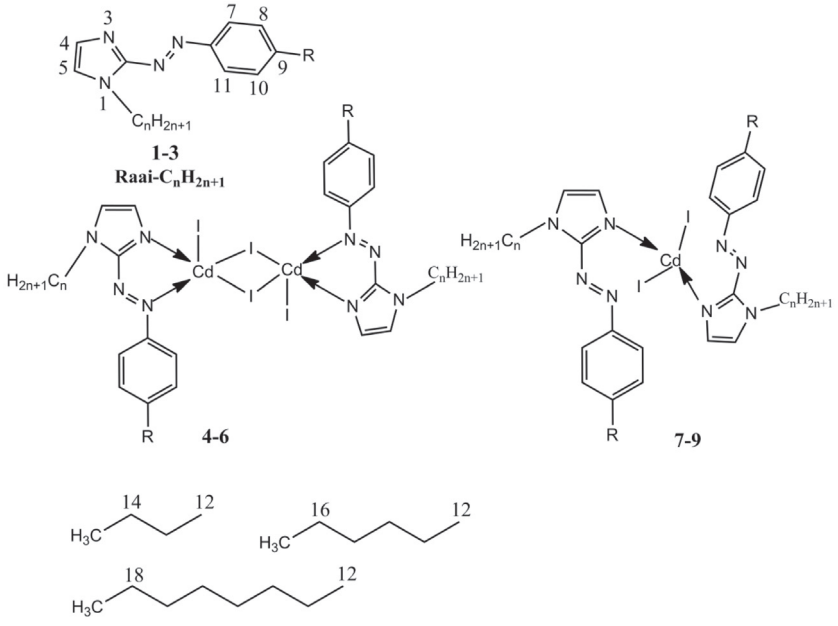

Haai-C_4H_9 (**1a/4a/7a**); Meaai-C_4H_9 (**1b/4b/7b**); Haai-C_6H_{13} (**2a/5a/8a**); Meaai-C_6H_{13} (**2b/5b/8b**); Haai-C_8H_{17} (**3a/6a/9a**); Meaai-C_8H_{17} (**3b/6b/9b**)

Scheme 2. The ligands Raai-C_nH_{2n+1} (**1–3**), the complexes [Cd(Raai-C_nH_{2n+1})(μ-I)I]$_2$ (**4–6**) and [Cd(Raai-C_nH_{2n+1})$_2$$I_2$] (**7–9**).

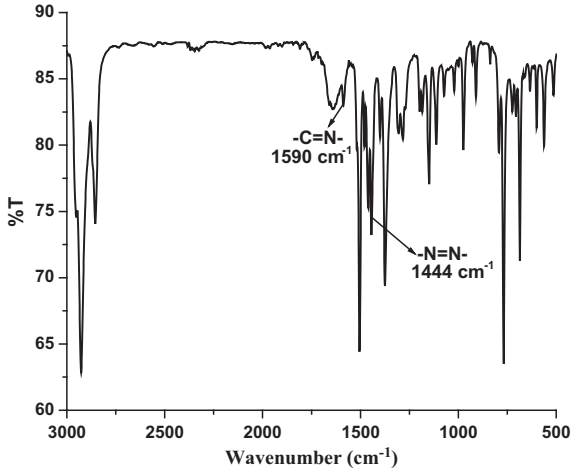

Fig. 1. FT-IR spectrum of [Cd(Meaai-C_6H_{13})$_2$$I_2$] (**8b**) using KBr disk.

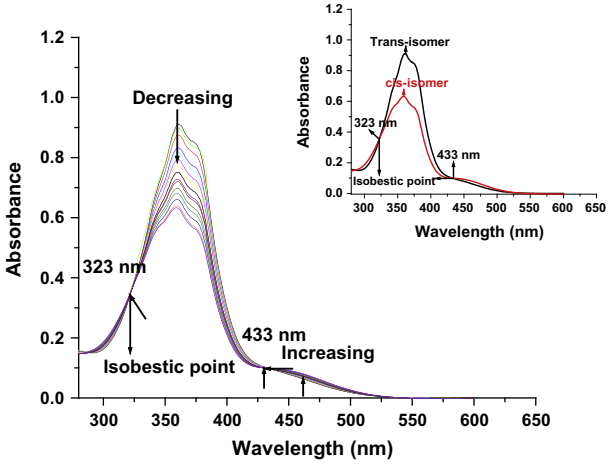

Fig. 3. Spectral changes of Haai-C_6H_{13} in MeOH upon repeated irradiation at 363 nm at 3 min. interval at 25 °C. Inset figure shows spectra of *cis* and *trans* isomer of the ligand: Haai-C_6H_{13}.

ν (C═N), 1562; UV–Vis λ_{max}, nm (ε, 10^3 M^{-1} cm^{-1}) in MeOH), 362 (27.62), 383 (25.95), 455 (3.7). [Cd(Meaai-C_8H_{17})$_2$$I_2$] (**9b**): Calculated for $C_{36}H_{52}N_8CdI_2$: C, 44.93; H, 5.39; N, 11.55%; Found: C, 45.21; H, 5.49; N, 11.74%. *m/z*+, 836.02. ^{1}H NMR (300 MHz, $CDCl_3$) δ 7.33 (2H, bs, 4,4′H),7.15 (2H, bs, 5,5′,H), 7.93 (4H, d, 7.2 Hz,7,7′,11,11′H), 7.34 (4H, d, 7.8 Hz, 8,8′,10,10′H), 2.46 (6H, s, 9,9′CH_3), 4.49 (4H, t, 6.8 Hz, 12,12′CH_2), 0.84 (6H, t, 6.4 Hz, 19,19′CH_3),1.91–1.36 (24H, m, 13–18,13′-18′CH_2). FT-IR (KBr, ν cm^{-1}) ν (N═N), 1412; ν (C═N), 1614; UV–Vis λ_{max}, nm (ε, 10^3 M^{-1} cm^{-1}) in MeOH), 366 (26.92), 385 (25.33), 449 (3.8).

Photometric measurements

Absorption spectra were taken with a PerkinElmer Lambda 25 UV/VIS Spectrophotometer in a 1 × 1 cm quartz optical cell maintained at 25 × C with a Peltier thermostat. The light source of a PerkinElmer LS 55 spectrofluorimeter was used as an excitation light, with a slit width of 10 nm. An optical filter was used to cut off overtones when necessary. The absorption spectra of the Z (*cis*) isomers were obtained by extrapolation of the absorption spectra of a *cis*-rich mixture for which the composition is known from ^{1}H NMR integration. Quantum yields (ϕ) were obtained by measuring initial E-to-Z isomerization rates (ν) in a well-stirred solution within the above instrument using the equation, $\nu = (\phi\, I0/V)(1-10^{-Abs})$ where I_0 is the photon flux at the front of the cell, V is the volume of the solution, and Abs is the initial absorbance at the irradiation wavelength. The value of I_0 was obtained by using azobenzene ($\phi = 0.11$ for π–π^* excitation [21]) under the same irradiation conditions.

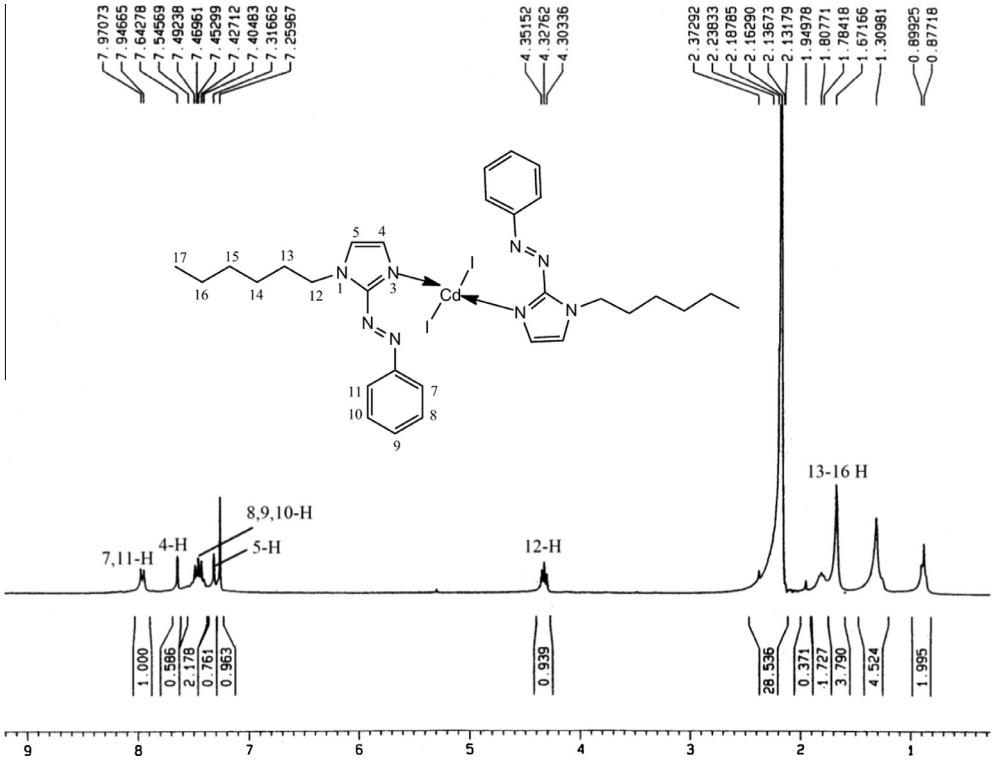

Fig. 2. ^{1}H NMR spectrum of [Cd(Haai-C_6H_{13})$_2$$I_2$] (**8a**) in $CDCl_3$.

The thermal Z-to-E isomerization rates were obtained by monitoring absorption changes intermittently for a Z-rich solution kept in the dark at constant temperatures (T) in the range from 298 to 313 K. The activation energy (E_a) and the frequency factor (A) were obtained from the Arrhenius plot, $\ln k = \ln A - E_a/RT$, where k is the measured rate constant, R is the gas constant, and T is temperature. The values of activation free energy (ΔG^*) and activation entropy (ΔS^*) were obtained through the relationships, $\Delta G^* = E_a - RT - T\Delta S^*$ and $\Delta S^* = [\ln A - 1 - \ln(k_B T/h)]/R$ where k_B and h are Boltzmann's and Plank's constants, respectively.

Theoretical calculations

All calculations were carried out using the Gaussian 03 program package [22]. Full geometry optimization of [Cd(Meaai-C_4H_9)(μ-I)I]$_2$ (**4b**) and [Cd(Haai-C_4H_9)$_2$I$_2$] (**7a**), were carried out using density functional theory (DFT) at the B3LYP level [23,24]. For C, H, N the 6-31G(d) basis set were assigned, while for Cd and I the LanL2DZ basis set with effective core potential were employed [25]. The Gauss View visualization program [26] has been used to draw the molecular functions. The vibrational frequency calculations were performed to ensure that the optimized geometries represent the local minima and there are only positive eigen values. Vertical electronic excitations based on B3LYP optimized geometries were computed using the time-dependent density functional theory (TD-DFT) formalism [27,28]. Gauss Sum was used to calculate the fractional contributions of various groups to each molecular orbital [29].

Results and discussion

The complexes and their formulation

1-Alkyl-2-(arylazo)imidazoles (Raai-C_nH_{2n+1} where n = 4 (**1**), 6 (**2**), 8 (**3**)) react with CdI_2 in 1:1 mol ratio and has isolated complexes of chemical formula [Cd(Raai-C_nH_{2n+1})(μ-I)I]$_2$ (**4–6**). The change of molar ratio of Raai-C_nH_{2n+1}: Cd(II) to 2:1 in MeOH has synthesized the complexes [Cd(Raai-C_nH_{2n+1})$_2$I$_2$] (**7–9**) (Scheme 2). The complexes are soluble in common organic solvents such as methanol, ethanol, acetonitrile, $CHCl_3$ (chloroform), CH_2Cl_2 (dichloroform), DMF (N,N-dimethylformamide) and are nonconducting. The mass spectra and microanalytical data support the composition of the complexes.

Spectral studies

The ligands, Raai-C_nH_{2n+1}, show ν(N=N) and ν (C=N) at 1390–1410 and 1610–1625 cm^{-1} while in the complexes moderately intense stretching at 1370–1420 and 1580–1695 cm^{-1} are due to ν(C=N) and ν(N=N), respectively (Fig. 1). In the complexes, stretching frequencies are shifted to lower frequency region which are in support of coordination of azo-N and imine-N to Cd(II) [5–10]. Other vibrations of the coordinated ligands in the complexes appear in the comparable position as in their free ligand spectra.

The ^{1}H NMR spectra of the ligands in $CDCl_3$ have been supported by published results [10]. The —N—CH_2 —$(CH_2)_n$—CH_3 shows a triplet for —CH_2— at 4.20 ppm, a triplet at 0.85 ppm. For —CH_3 group and a multiplet for —$(CH_2)_n$— at 1.18–1.80 ppm (Fig. 2). Imidazolyl 4- and 5-H appear as broad singlet at 7.20–7.28 and 7.10–7.15 ppm, respectively. Broadening may be due to rapid proton exchange between these imidazolyl protons/solvents. The aryl protons (7-H to 11-H) are upfield shifted on going from phenylazo (**a**) to *p*-tolylazo (**b**). Data reveal that the signals in the spectra of the complexes are shifted to downfield side relative to free ligand values. This supports the coordination of ligand to Cd(II). Imidazolyl protons (4,5-H) suffer downfield shifting by a small amount, 0.05–0.15 ppm compared to the free ligand position. This supports the binding of imidazolyl-N to Cd(II).

UV–Vis spectra and photochromism

The absorption spectra of the ligands show transitions at 340–370 nm with a molar absorption coefficient in the order of 10^3 M^{-1} cm^2 with a weak band at 450–455 nm. The complexes show absorption band around 355–370 nm with a molar absorption coefficient on the order of 10^3 M^{-1} cm^2 (n–π^*) at 450–460 nm.

The UV light irradiation to a MeOH solution of the complexes show the change of absorption spectrum (Fig. 3); the intense peak at λ_{max} decreases, which is accompanied by a slight increase at the tail portion (longer λ) of the spectrum around 510 nm until a stationary state (Photostationary State-I, PSS-I) is reached. Following irradiation at the newly appeared longer wavelength peak reverses the course of the reaction and the original spectrum is recovered up to a point, which is another photostationary state (Photostationary State-II, PSS-II) under irradiation at the longer wavelength peak. The quantum yields of the E-to-Z (*trans*-to-*cis*) photoisomerization were determined using those of azobenzene as a standard and the results are tabulated in Table 1. Thermal Z-to-E (*cis*-to-*trans*) isomerization rates of these complexes in MeOH at

Table 1
Results of photochromism, rate of conversion and quantum yields[a] of [Cd(Raai-C_nH_{2n+1})(μ-I)I]$_2$ (**4–6**) and [Cd(Raai-C_nH_{2n+1})$_2$I$_2$] (**7–9**) upon UV light irradiation.

Compounds	λ_{π,π^*} (nm)	Isosbestic point (nm)	Rate of E → Z conversion × 10^8 (s^{-1})	$\phi_{E\to Z}$
[Cd(Haai-C_4H_9)(μ-I)I]$_2$ (**4a**)	365	324.435	2.84	0.097
[Cd(Meaai-C_4H_9)(μ-I)I]$_2$ (**4b**)	366	323.433	1.84	0.096
[Cd(Haai-C_6H_{13})(μ-I)I]$_2$ (**5a**)	366	328.437	1.82	0.092
[Cd(Meaai-C_6H_{13})(μ-I)I]$_2$ (**5b**)	367	333.436	1.80	0.089
[Cd(Haai-C_8H_{17})(μ-I)I]$_2$ (**6a**)	367	331.432	1.73	0.086
[Cd(Meaai-C_8H_{17})(μ-I)I]$_2$ (**6b**)	365	334.436	1.73	0.087
[Cd(Haai-C_4H_9)$_2$I$_2$] (**7a**)	367	320.437	2.70	0.138
[Cd(Meaai-C_4H_9)$_2$I$_2$] (**7b**)	367	325.435	2.81	0.140
[Cd(Haai-C_6H_{13})$_2$I$_2$] (**8a**)	366	323.444	2.81	0.139
[Cd(Meaai-C_6H_{13})$_2$I$_2$] (**8b**)	368	331.433	2.81	0.138
[Cd(Haai-C_8H_{17})$_2$I$_2$] (**9a**)	362	330.431	2.43	0.124
[Cd(Meaai-C_8H_{17})$_2$I$_2$] (**9b**)	368	332.435	2.38	0.125

[a] Ligand – λ(Irradiation), rate of E → Z conversion × 10^9 (s^{-1}) and 10 × $\phi_{E\to Z}$ for ligands: Haai-C_4H_9 (**1a**) – 363 nm, 36.01, 1.90; Meaai-C_4H_9 (**1b**) – 362 nm, 35.71, 1.87; Haai-C_6H_{13} (**2a**) – 363 nm, 34.92, 1.81; Meaai-C_6H_{13} (**2b**) – 361 nm, 34.09, 1.79; Haai-C_8H_{17} (**3a**) – 364 nm, 33.76, 1.69; Meaai-C_8H_{17} (**3b**) – 365 nm, 28.42, 0.97. Data collected from Ref. [10].

Table 2
Rate, activation parameters and thermodynamic data for Z (cis) → E (*trans*) of [Cd(Raai-C_nH_{2n+1})(μ-I)I]$_2$ (**4–6**) and [Cd(Raai-C_nH_{2n+1})$_2$I$_2$] (**7–9**)[a] in MeOH.

Compounds	Temp (K)	Rate of thermal c → t conversion × 10^4 (s^{-1})	E_a, kJ mol^{-1}	ΔH^* kJ mol^{-1}	ΔS^* J mol^{-1} K^{-1}	ΔG^{*c} kJ mol^{-1}
[Cd(Haai-C_4H_9)(μ-I)I]$_2$ (**4a**)	298	3.34	35.64	33.10	−200.13	94.23
	303	4.53				
	308	5.59				
	313	6.69				
[Cd(Meaai-C_4H_9)(μ-I)I] (**4b**)	298	3.49	33.93	31.39	−215.43	94.15
	303	4.82				
	308	5.73				
	313	6.82				
[Cd(Haai-C_6H_{13})(μ-I)I] (**5a**)	298	3.57	33.33	30.79	−207.39	94.14
	303	4.67				
	308	5.73				
	313	6.82				
[Cd(Meaai-C_6H_{13})(μ-I)I] (**5b**)	298	3.53	33.21	30.63	−208.00	94.18
	303	4.63				
	308	5.68				
	313	6.72				
[Cd(Haai-C_8H_{17})(μ-I)I] (**6a**)	298	3.58	32.74	30.21	−209.24	94.13
	303	4.78				
	308	5.79				
	313	6.78				
[Cd(Meaai-C_8H_{17})(μ-I)I] (**6b**)	298	3.68	31.18	28.65	−214.34	94.14
	303	4.78				
	308	5.60				
	313	6.82				
[Cd(Haai-C_4H_9)$_2$I$_2$] (**7a**)	298	3.38	39.40	36.86	−187.18	94.04
	303	4.92				
	308	6.38				
	313	7.21				
[Cd(Meaai-C_4H_9)$_2$I$_2$] (**7b**)	298	3.52	32.30	29.76	−210.97	94.21
	303	4.63				
	308	5.45				
	313	6.67				
[Cd(Haai-C_6H_{13})$_2$I$_2$] (**8a**)	298	3.52	30.05	27.52	−216.92	93.79
	303	4.78				
	308	6.13				
	313	7.13				
[Cd(Meaai-C_6H_{13})$_2$I$_2$] (**8b**)	298	3.67	36.66	34.12	−196.12	94.04
	303	4.64				
	308	6.23				
	313	7.31				
[Cd(Haai-C_8H_{17})$_2$I$_2$] (**9a**)	298	3.49	32.86	30.35	−209.21	94.21
	303	4.43				
	308	5.29				
	313	6.67				
[Cd(Meaai-C_8H_{17})$_2$I$_2$] (**9b**)	298	3.48	32.29	30.35	−209.21	94.26
	303	4.51				
	308	5.32				
	313	6.59				

[a] Thermal data [10] of ligands E_a, (kJ mol^{-1}), ΔH (kJ mol^{-1}), ΔS (J mol^{-1} K^{-1}), ΔG (kJ mol^{-1}) are as given: **1a**, 88.20, 85.66, −43.27, 98.9; **1b**, 88.47, 85.93, −37.96, 97.53; **2a**, 91.73, 89.19, −30.09, 98.36; **2b,** 92.11, 89.57, −25.12, 98.38; **3a**, 93.38, 90.85, −23.83, 98.13; **3b**, 93.66, 91.12, −19.45, 97.07.

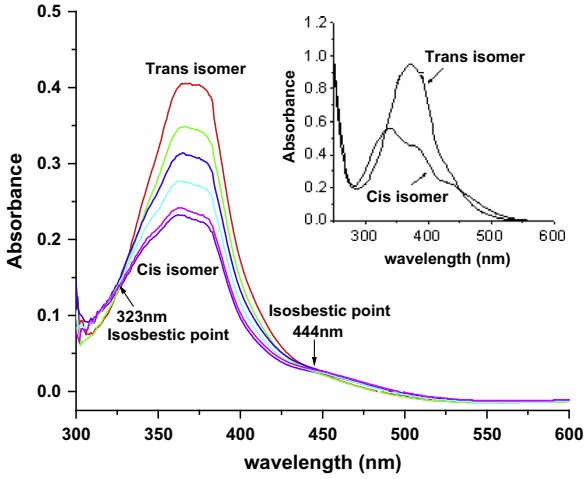

Fig. 4. Spectral changes of [Cd(Haai-C_6H_{13})$_2$I$_2$] (**8a**) in MeOH upon repeated irradiation at 366 nm at 5 min interval at 25 °C.

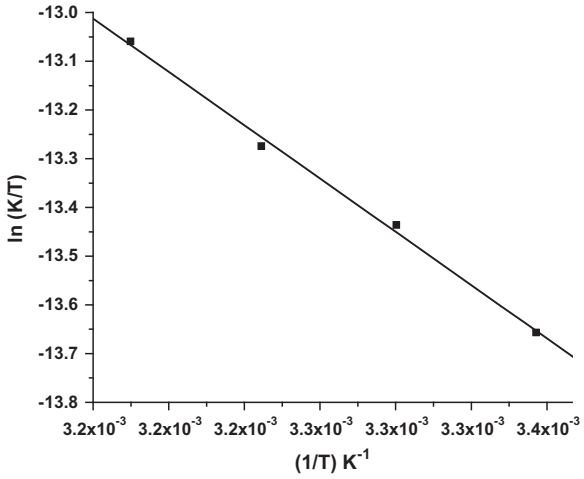

Fig. 5. The Eyring plots of rate constants of Z-to-E isomerisation of [Cd(Haai-C_8H_{17})$_2$I$_2$] (**9a**) in MeOH at different temperatures 298–313 K.

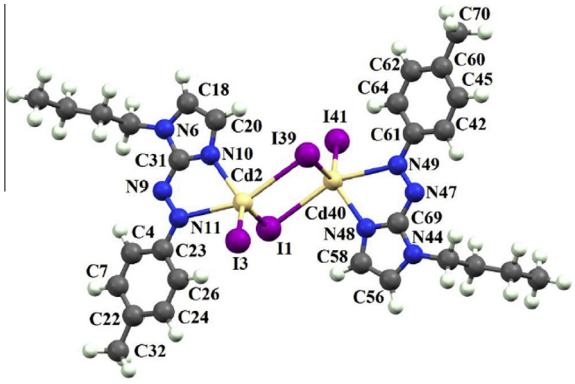

Fig. 6. Optimized structure of $[Cd(Meaai\text{-}C_4H_9)(\mu\text{-}I)I]_2$ (**4b**) drawn by using DFT-B3LYP function.

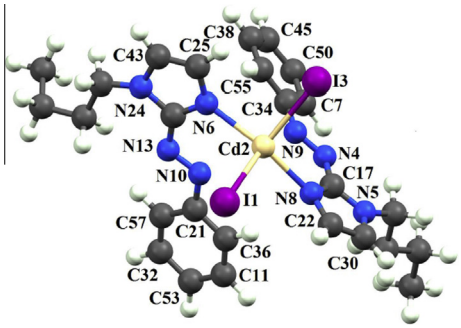

Fig. 7. Optimized structure of $[Cd(Haai\text{-}C_4H_9)_2I_2]$ (**7a**) drawn by using DFT-B3LYP function.

298–313 K are given in Table 2. It is observed that upon irradiation with UV light E-to-Z photoisomerisation proceeded and the Z-molar ratio is reached to ~75%. The absorption spectra of the E-ligands changed with isosbestic points upon excitation (Fig. 4) into the Z-isomer and also in case of respective complexes. The quantum yields were measured for the E-to-Z ($\phi_{E\rightarrow Z}$) photoisomerisation of these ligands and complexes in MeOH on irradiation of UV wavelength (Tables 1 and 2). The $\phi_{E\rightarrow Z}$ values are significantly dependent on molar mass and increase in mass of the molecule reduces the rate of isomerisation *trans*-to-*cis*. In the complexes the $\phi_{E\rightarrow Z}$ values are significantly less than that of free ligand data. It may be due to the presence of coordinated CdI_2 motif that heavily increases molecular weight of the complex unit and may interfere with the motion of the —N=N—Ar moiety and the photo bleaching efficiency of iodo group which may snatch out energy from π–π^* excited state. These may cause very fast deactivation other than photochromic route. The rotor volume has significant influence on the isomerisation rate and quantum yields.

The E-to-Z isomerisation is carried out at variable temperature at 298–313 K followed by UV–Vis spectroscopy in MeOH. The Eyring plots in the range 298–313 K given a linear graph from which the activation energy was obtained (Table 2, Fig. 5). In the complexes, the E_as are severely reduced which means faster *cis*-to-*trans* thermal isomerisation of the complexes. The entropy of activation (ΔS^*) are high negative in the complexes than that of free ligand. This is also in support of increase in rotor volume in the complexes.

DFT computation optimized structures and frontier molecular orbitals

Optimized counterparts of $[Cd(Meaai\text{-}C_4H_9)(\mu\text{-}I)I]_2$ (**4b**) and $[Cd(Haai\text{-}C_4H_9)_2I_2]$ (**7a**) can be seen from Figs. 6 and 7. The calculated bond distances, bond angles and torsion angles of the compounds are listed in Table 3. The structure of **4b** shows iodo bridged Cd_2I_2 fragment and Meaai-C_4H_9 serves as N,N′ end capping agent and a non-bridged–I atom lies in a semi-axial position. The bridged Cd_2I_2 is unsymmetric tetra-atomic plane; the calculated bond distances are Cd(2)—I(1), 2.95288 Å; Cd(2)—I(39), 3.15001 Å; Cd(40)—I(1), 3.14977 Å; Cd(40)—I(39), 2.94992 Å. The Cd(2)—N(10), 2.3082 is shorter than Cd—N(11), 2.7440 Å which theoretically accounts the stronger interaction between Cd(II) and N(imidazole) than Cd(II) and N(azo). The calculated geometry of $[Cd(Haai\text{-}C_4H_9)_2I_2]$ (**7a**) is tetrahedral with CdN_2I_2 coordination sphere. The Cd(2)—N(6)/N(9) distances are 2.3692 and 2.3413 Å; the Cd—I distances are 2.9034 and 2.8873 Å. The azo distance, N(9)—N(11), 1.2984 Å in **4b** is comparable with calculated distance of **7a** (N(4)—N(9), 1.2971 Å and N(10)—N(13), 1.3024 Å) chelated geometry. This has been examined with structurally characterized

Table 3
Optimized geometries of the $[Cd(Meaai\text{-}C_4H_9)(\mu\text{-}I)I]_2$ (**4b**) and $[Cd(Haai\text{-}C_4H_9)_2I_2]$ (**7a**).

Bond distances (Å)		Bond angles (°)		Torsion angles (°)	
[Cd(Meaai-C_4H_9)(μ-I)I]$_2$ ***(4b)***					
Cd(2)—I(1)	2.9529	I(1)—Cd(2)—I(39)	91.6711	N(10)—Cd(2)—I(39)—Cd(40)	−104.41137
Cd(2)—I(39)	3.1500	I(1)—Cd(2)—I(3)	125.3893	N(11)—Cd(2)—I(1)—Cd(40)	153.37366
Cd(2)—I(3)	2.8076	I(3)—Cd(2)—N(11)	97.1651	Cd(2)—N(11)—N(9)—C(31)	−5.54197
Cd(2)—N(11)	2.7440	N(11)—Cd(2)—N(10)	66.0707	Cd(2)—N(10)—C(31)—N(9)	3.80127
Cd(2)—N(10)	2.3082	I(39)—Cd(2)—N(10)	89.5846	I(3)—Cd(2)—I(39)—Cd(40)	128.04565
N(9)—N(11)	1.2984	Cd(2)—N(11)—N(9)	112.0221	I(3)—Cd(2)—I(1)—Cd(40)	−110.91065
Cd(40)—I(1)	3.1498	I(1)—Cd(40)—I(39)	91.7315	N(49)—Cd(40)—I(39)—Cd(2)	−154.12317
Cd(40)—I(39)	2.9499	I(39)—Cd(40)—I(41)	124.7418	N(48)—Cd(40)—I(1)—Cd(2)	106.79135
Cd(40)—I(41)	2.8094	I(41)—Cd(40)—N(49)	96.6771	Cd(40)—N(49)—N(47)—C(69)	4.81896
Cd(40)—N(49)	2.7431	N(48)—Cd(40)—N(49)	66.0789	Cd(40)—N(48)—C(69)—N(47)	−1.93861
Cd(40)—N(48)	2.3084	I(1)—Cd(40)—N(48)	89.3309	I(41)—Cd(40)—I(1)—Cd(2)	−126.44121
N(47)—N(49)	1.2984	Cd(40)—N(49)—N(47)	112.1189	I(41)—Cd(40)—I(39)—Cd(2)	110.12473
*[Cd(Haai-C_4H_9)$_2$I$_2$] (**7a**)*					
Cd(2)—I(1)	2.9034	N(6)—Cd(2)—N(8)	154.5969	I(1)—Cd(2)—N(8)—C(17)	164.46802
Cd(2)—I(3)	2.8873	N(8)—Cd(2)—I(3)	99.4804	I(3)—Cd(2)—N(8)—C(17)	−70.48212
Cd(2)—N(6)	2.3692	N(6)—Cd(2)—I(1)	95.0221	N(8)—C(17)—N(4)—N(9)	3.52290
Cd(2—N(8)	2.3413	I(1)—Cd(2)—I(3)	123.2986	I(1)—Cd(2)—N(6)—C(52)	−69.78039
N(6)—C(52)	1.3316	N(6)—Cd(52)—N(24)	33.3828	I(3)—Cd(2)—N(6)—C(52)	166.23892
N(24)—C(52)	1.4382	C(5)—N(6)—C(52)	107.9851	N(6)—C(52)—N(13)—N(10)	3.20844
N(10)—N(13)	1.3024	C(52)—N(24)—C(43)	104.7754		
N(8)—C(17)	1.3523	C(22)—N(8)—C(17)	106.8204		
N(5)—C(17)	1.3838	N(8)—C(17)—N(24)	110.3968		
N(4)—N(9)	1.2971	C(17)—N(5)—C(30)	106.9896		

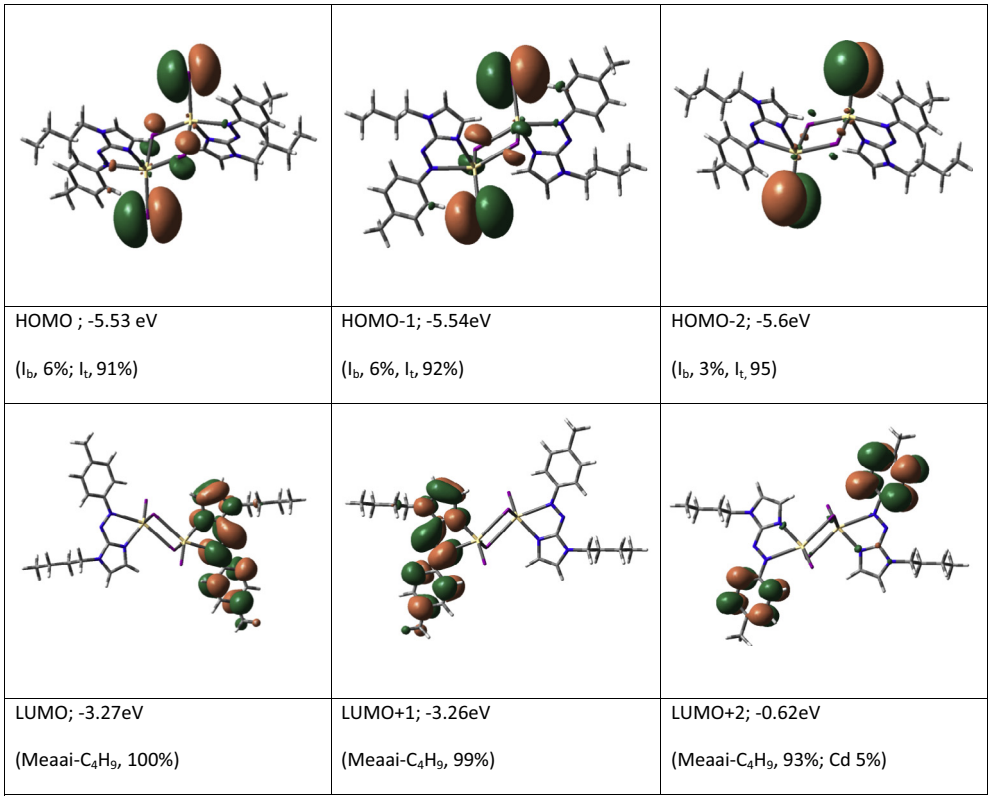

Fig. 8. Contour plots of some MOs of [Cd(Meaai-C_4H_9)(μ-I)I]$_2$ (**4b**) (data in braces suggest % contribution of part function to MOs) (I_b refers to bridging-I; I_t refers to terminal-I).

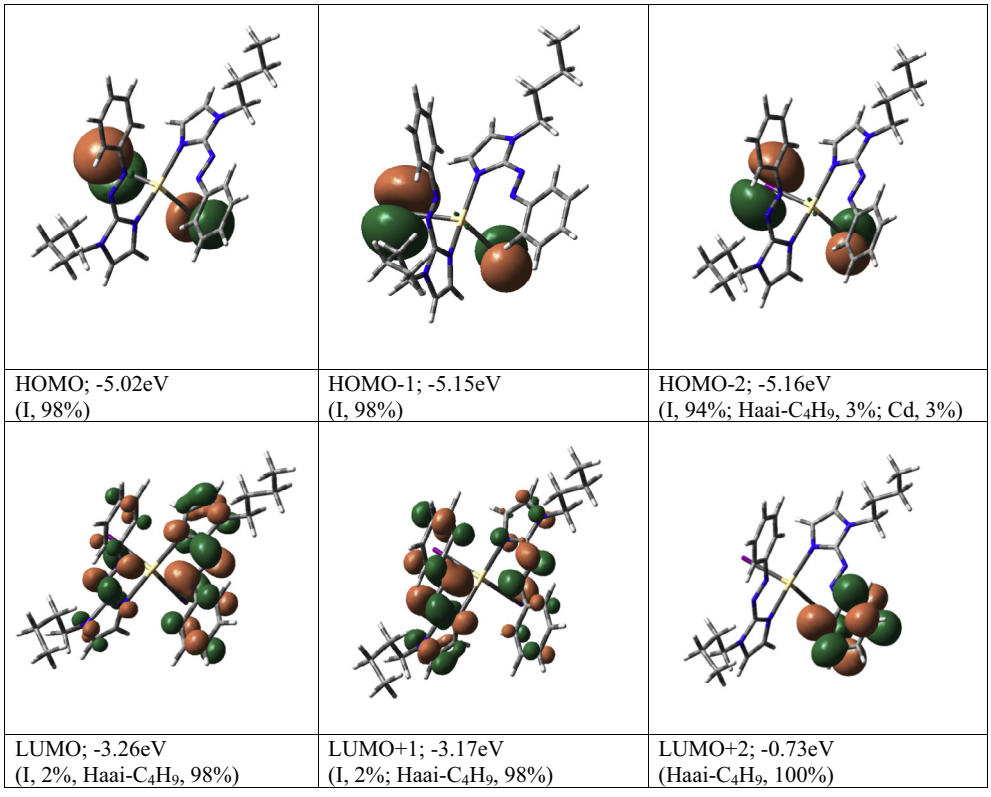

Fig. 9. Contour plots of some MOs of [Cd(Haai-C_4H_9)$_2$I$_2$] (**7a**) (data in braces suggest % contribution of part function to MOs).

Table 4
The spectral transitions calculated by TD-DFT computation of $[Cd(Meaai\text{-}C_4H_9)(\mu\text{-}I)I]_2$ (**4b**) and $[Cd(Haai\text{-}C_4H_9)_2I_2]$ (**7a**) in gaseous state.

Excitation energy (eV)	Wavelength (nm)	*f*	Key transitions	Character
$[Cd(Meaai\text{-}C_4H_9)(\mu\text{-}I)I]_2$ ***(4b)***				
2.9753	416.72	0.1986	(27%) HOMO−8 → LUMO+1	X_bLCT
3.0101	411.90	0.1702	(22%) HOMO−5 → LUMO	X_bLCT
3.0419	407.59	0.9925	(26%) HOMO−8 → LUMO+1	X_bLCT
3.1859	389.17	0.1052	(74%) HOMO−10 → LUMO+1	ILCT
4.5132	274.71	0.0799	(44%) HOMO−21 → LUMO	ILCT
5.2857	234.57	0.2506	(21%) HOMO−6 → LUMO+2	X_bLCT
$[Cd(Pai\text{-}C_4H_9)_2I_2]$ ***(7a)***				
2.9278	423.47	0.0312	(33%) HOMO−8 → LUMO	ILCT
3.1252	396.72	0.3658	(33%) HOMO-6 → LUMO	ILCT
3.1351	395.47	0.1129	(70%) HOMO−7 → LUMO+1	ILCT
3.2056	386.77	0.8719	(30%) HOMO−6 → LUMO+1	ILCT
3.5235	351.88	0.0750	(51%) HOMO−10 → LUMO	ILCT
4.5012	275.45	0.0378	(73%) HOMO−15 → LUMO	ILCT

ILCT: Intraligand charge transfer transition; X_bLCT: terminal-I to $\pi^*(Raai\text{-}C_nH_{2n+1})$ charge transfer transition.

Cd(II) and Hg(II) complexes of Raai-C_nH_{2n+1} [8–10]. The chelate angle (∠N(10) − Cd(2) − N(11), 66.0707°) and other values of bond angles agree well with distorted penta-coordinated geometry (Table 3) [8–10].

The energy of molecular orbitals HOMO, HOMO-1 and HOMO-2 of **4b** are closely spaced (E_{HOMO}, −5.53 eV; E_{HOMO-1}, −5.54 eV; E_{HOMO-2}, −5.6 eV). The energy of the molecular orbitals (MOs) depends on number of coordinated Raai-$C_{10}H_{21}$ attached to Cd(II). In **7a** the MOs are placed slightly higher than that of **4b**; E_{HOMO}, −5.02 eV; E_{HOMO-1}, −5.15 eV; E_{HOMO-2}, −5.16 eV. Unoccupied MOs LUMO (E_{LUMO}, −3.27 eV) and LUMO + 1 (E_{LUMO+1}, −3.25 eV) are closely spaced while LUMO + 2 (E_{LUMO+2}, 3.27 eV) and higher energy MOs are at very high energy position (>−0.6 eV). With increase in number of coordinated ligand with Cd(II) the energy of occupied MOs are decreasing. The occupied MOs of **4b** are mainly composed of terminal-I (I_t) (>90%) and the unoccupied MOs have >80% Meaai-$C_{10}H_{21}$ characteristics. Similar observations have been calculated for **7a.** Representative MOs are shown in Figs. 8 and 9.

The electronic transitions in the complexes may be associated with intra-ligand π(azoimine) → π*(azoimine) and/or I_t (terminal-I), I_b (bridging-I) → π*(azoimine) charge transfer transitions (Table 4). The $I_t \rightarrow \pi^*$ transition may appear 260–280 nm while $I_b \rightarrow \pi^*$ may be at 235–250 nm. Strong π–π* transitions (H-9 to L with a charge transfer character) are expected around (415 nm).

Conclusion

The complexes, $[Cd(Raai\text{-}C_nH_{2n+1})(\mu\text{-}I)I]_2$ and $[Cd(Raai\text{-}C_nH_{2n+1})_2I_2]$ are used to examine the effect of light irradiation on the structure of coordinated Raai-C_nH_{2n+1} (1-alkyl-2-(arylazo)imidazoles, $n = 4, 6, 8$). Rate and quantum yield of photoisomerisation, E-to-Z (*trans*-to-*cis*) depends on the molar mass of the complexes; rate decreases with increase in mass. The reverse transformation, Z-to-E (*cis*-to-*trans*) has been carried out under thermal treatment. DFT optimized structures of $[Cd(Meaai\text{-}C_4H_9)(\mu\text{-}I)I]_2$ (**4b**) and $[Cd(Haai\text{-}C_4H_9)_2I_2]$ (**7a**) show comparable to those of reported structures and the molecular functions generated from these structures have been used to explain the spectroscopic properties. The structural characterization of these complexes has been carried out by spectroscopic data.

Acknowledgements

Financial support from the West Bengal Department of Science & Technology, Kolkata, India (Sanction No. 228/1(10)/(Sanc.)/ST/P/S&T/9G-16/2012) and the Council of Scientific and Industrial Research (CSIR, Sanction No. 01(2731)/13/EMR-II,), New Delhi, India are gratefully acknowledged. One of us (C. Sen) is thankful to the University Grants Commission, New Delhi, India for fellowship.

Appendix A. Supplementary material

Supplementary data associated with this article can be found, in the online version, at http://dx.doi.org/10.1016/j.saa.2014.08.094.

References

[1] 1.N. Tamaoki, New frontiers in photochromism, in: M. Irie, Y. Yokoyama, T. Seki (Eds.), Springer, Japan, 2013.
[2] H. Durr, H. Bouas-Laurent (Eds.), Photochromism. Molecules and Systems, Elsevier, Amsterdam, 2003.
[3] J. Otsuki, K. Suwa, K. Narutaki, C. Sinha, I. Yoshikawa, K. Araki, J. Phys. Chem. A 109 (2005) 8064–8069.
[4] K.K. Sarker, B.G. Chand, J. Cheng, T.-H. Lu, C. Sinha, Inorg. Chem. 46 (2007) 670–680.
[5] D. Mallick, K.K. Sarker, P. Datta, T.K. Mondal, C. Sinha, Inorg. Chim. Acta 387 (2012) 352–360.
[6] P. Datta, D. Mallick, T.K. Mondal, C. Sinha, Polyhedron 71 (2014) 47–61.
[7] S. Saha (Halder), P. Raghavaiah, C. Sinha, Polyhedron 46 (2012) 25–32.
[8] K.K. Sarker, D. Sardar, K. Suwa, J. Otsuki, C. Sinha, Inorg. Chem. 46 (2007) 8291–8301.
[9] 9.S. Saha (Halder), B.G. Chand, J.-S. Wu, T.-H. Lu, P. Raghavaiah, C. Sinha, Polyhedron 46 (2012) 81–89.
[10] D. Mallick, A. Nandi, S. Datta, K.K. Sarker, T.K. Mondal, C. Sinha, Polyhedron 31 (2012) 506–514.
[11] J.A. Mondal, G. Saha, C. Sinha, D.K. Palit, Phys. Chem. Chem. Phys. 14 (2012) 13027–13034.
[12] A. Nandi, C. Sen, D. Mallick, R.K. Sinha, C. Sinha, Adv. Mater. Phys. Chem. 3 (2013) 133–145.
[13] H.M.D. Bandarab, S.C. Burdette, Chem. Soc. Rev. 41 (2012) 809–1825.
[14] 14.T. Schultz, J. Quenneville, B. Levine, A. Toniolo, T.J. Martınez, S. Lochbrunner, M. Schmitt, J.P. Shaffer, M.Z. Zgierski, A. Stolow, J. Am. Chem. Soc. 125 (2003) 8098–8099.
[15] Photo-reactive materials for ultrahigh density optical memory, (Ed: M. Irie) Elsevier, Amsterdam, 1994.
[16] M. Irie, Chem. Rev. 100 (2000) 1683–1684.
[17] Molecular switches, (Ed. B. Feringa) Wiley-VCH, 2001.
[18] P. Gayen, T.K. Misra, C. Sinha, J. Spectrosc. Dyn. 4 (2014) 27–35.
[19] P. Gayen, C. Sinha, Spectrochim. Acta Part A 104 (2013) 477–485.
[20] P. Gayen, K.K. Sarker, C. Sinha, Colloids Surf. A 429 (2013) 60–66.
[21] G. Zimmerman, L. Chow, U. Paik, J. Am. Chem. Soc. 80 (1958) 3528–3531.
[22] Gaussian 03, Revision C.02, M.J. Frisch, G.W. Trucks, H.B. Schlegel, G.E. Scuseria, M.A. Robb, J.R. Cheeseman, J.A. Montgomery, Jr. T. Vreven, K.N. Kudin, J.C. Burant, J.M. Millam, S.S. Iyengar, J. Tomas, V. Barone, B. Mennucci, M. Cossi, G. Scalmani, N. Rega, G. A. Petersson, H. Nakatsuji, M. Hada, M. Ehara, K. Toyota, R. Fukud, J. Hasegawa, M. Ishida, T. Nakajima, Y. Honda, O. Kitao, H. Nakai, M. Klene, X. Li, J.E. Knox, H.P. Hratchian, J.B. Cross, V. Bakken, C. Adamo, J. Jaramillo, R. Gomperts, R.E. Stratmann, O. Yazyev, A.J. Austin, P. Cammi, C. Pomelli, J.W. Ochterski, P.Y. Ayala, K. Morokuma, G.A. Voth, P. Salvador, J.J. Dannenberg, V.G. Zakrzewski, S. Dapprich, A.D. Daniels, M.C. Strain, O. Farkas, D.K. Malick, A.D. Rabuck, K. Raghavachari, J.B. Foresman, J.V. Ortiz, Q. Cui, A.G. Baboul, S. Clifford, J. Cioslowski, B.B. Stefanov, G. Liu, A. Liashenko, P. Piskorz, I. Komaromi, R.L. Martin, D.J. Fox, T. Keith, M.A. Al-Laham, C.Y. Peng, A.

Nanayakkara, M. Challacombe, P.M.W. Gill, B. Johnson, W. Chen, M.W. Wong, C. Gonzalez, J.A. Pople, Gaussian Inc., Wallingford CT, 2004.
[23] C. Lee, W. Yang, R.G. Parr, Phys. Rev. B 37 (1988) 785–789.
[24] A.D. Becke, J. Chem. Phys. 98 (1993) 5648–5652.
[25] P.J. Hay, W.R. Wadt, J. Chem. Phys. 82 (1985) 270–283.
[26] N.M. O'Boyle, J.G. Vos, GaussSum 1.0; Dublin City University: Dublin, Ireland, 2005.
[27] R. Bauernschmitt, R. Ahlrichs, Chem. Phys. Lett. 256 (1996) 454–464.
[28] M.E. Casida, C. Jamorski, K.C. Casida, D.R. Salahub, J. Chem. Phys. 108 (1998) 4439–4449.
[29] N.M. O'Boyle, A.L. Tenderholt, K.M. Langner, J. Comput. Chem. 29 (2008) 839–845.